

# PARTICLE DYNAMICS OF MONO-DOMAIN PARTICLES IN MAGNETIC PARTICLE IMAGING

JÜRGEN WEIZENECKER

*Department of Electrical Engineering, University of Applied Science,  
Moltkestrasse 30, 76133 Karlsruhe, Germany  
Email: juergen.weizenecker@hs-karlsruhe.de*

BERNHARD GLEICH, JÜRGEN RAHMER, JÖRN BORGERT

*Philips Research Europe – Hamburg,  
Röntgenstraße 24-26, 22335 Hamburg, Germany  
Email: bernhard.gleich@philips.com*

In this report we present a detailed model of Brownian, Néel and combined rotation of magnetic mono domain particles in Magnetic Particle Imaging (MPI)<sup>5</sup>. The magnetization and rotational movement is predicted using a set of Langevin equations. The stochastic differential equations were solved numerically and applied to MPI for a simple sequence. At 25 kHz and with moderate anisotropies, the Néel rotation dominates the signal. Nevertheless, the Brownian motion modulates the signal in a model of combined motion.

## 1. INTRODUCTION

Magnetic Particle Imaging (MPI) does not provide any natural contrast and thus needs a tracer to perform imaging, the performance of which is of crucial importance. In order to understand the behaviour of the tracer in the various applied magnetic fields a suitable model has to be provided. It has been shown, that the simple Langevin Theory of magnetism is capable of describing the important features of the imaging process<sup>7,13</sup>. In a real experiment, of course, the tracer will always contain different types of particles (in terms of size and anisotropy). Nevertheless, the above-mentioned theory can still be used as an approximation in which distributions of parameters are modelled by effective values, like mean diameter and magnetization<sup>8</sup>.

However, in order to evaluate ways to increase the performance of the particles and to understand experimental data, a more detailed model has to be provided. The model should contain relevant input parameters like particle diameter, arbitrary time

varying magnetic fields, magnetic particle anisotropy, magnetization relaxation, and thermodynamic equilibrium.

There are two relevant mechanisms to change the magnetization of magnetic particles in an external field (figure 1). The first one is based on the reorientation of the magnetic particles and is named Brownian rotation. The second one is based on the change of magnetization in the fixed particle and is named Néel rotation. This report will present a detailed theory, which describes both effects separately, as well as in combination.

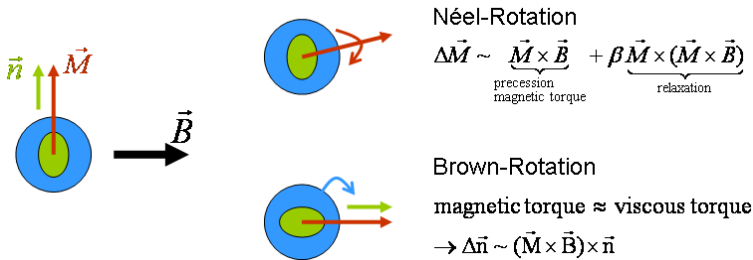


**Fig. 1.** Magnetization change of a single particle. In case of Néel rotation, the magnetization changes inside the particle. The magnetization can also change due to particle reorientation, referred to as Brownian rotation.

## 2. THEORY

### 2.1. Brownian Rotation

The behaviour of a spherical magnetic particle for the case of Brownian rotation in an external field  $\vec{B}$  can be described<sup>5</sup> by

$$\frac{d\vec{n}}{dt} = \frac{V_{core}M_s}{6\eta V_{Hydro}} (\vec{n} \times \vec{B}) \times \vec{n} + \vec{N}(t) \times \vec{n}$$

Here the unit vector  $\vec{n}$  represents a fixed direction of the particle; its direction is the same as the direction of the magnetization of the particle, as within the particle, the magnetization is assumed to be fixed. The parameter  $\eta$  is the viscosity,  $V_{core}(V_{Hydro})$  is the core (hydrodynamic) volume of the particle, and  $M_s$  is the saturation magnetization of the particle. The term  $\vec{N}(t)$  is proportional to a random torque describing the thermal impact on the microscopic particles. The above equation is quite similar to the differential description of Brownian motion of particles. For the components of the random vector field the following conditions are valid.

$$\langle \mathbf{N}_i(t) \rangle = 0 \quad \langle \mathbf{N}_i(t) \mathbf{N}_j(t') \rangle = \frac{2k_B T}{6\eta V_{Hydro}} \delta(t-t') \delta_{ij} \quad i, j = 1, 2, 3$$

Such an equation is named Langevin equation and describes the particle direction by a stochastic differential equation. It can be interpreted in the Ito or Stratonovitch calculus<sup>3,6</sup>. The numerical solution will in general differ depending on the interpretation. For physical reasons<sup>3</sup> we chose the Stratonovitch interpretation and transform the above equation according to the transformation rules between Stratonovitch and Ito calculus<sup>6</sup>. This adds an additional diffusion term and the final equation becomes

$$d\vec{n} = \left[ \frac{V_{core} M_s}{6\eta V_{Hydro}} (\vec{n} \times \vec{B}) \times \vec{n} - \frac{2k_B T}{6\eta V_{Hydro}} \vec{n} \right] dt + \sqrt{\frac{2k_B T}{6\eta V_{Hydro}}} d\vec{W} \times \vec{n} \quad (1)$$

For a numerical solution,  $d\vec{n}$ ,  $dt$ ,  $d\vec{W}$  are replaced by  $\vec{n}(t_k + \Delta t) - \vec{n}(t_k)$ ,  $\Delta t$  and  $\vec{W} \sqrt{\Delta t}$ , respectively. The random numbers  $W_j$ ,  $j = 1, 2, 3$  have zero mean value and unit standard deviation. The three coupled stochastic differential equations are solved using a Heun<sup>11</sup> scheme. To derive a mean value, the differential equations have to be solved multiple times and the results averaged. As in this case the single particle magnetization is assumed to always face in particle direction  $\vec{n}$ , the mean (single particle) magnetization for  $P$  solutions of equation (1) is

$$\frac{1}{P} \sum_{i=1}^P M_s \vec{n}_i$$

The mean (single particle) magnetic moment is obtained by multiplication with the particle core volume  $V_{core}$ . The first part of equation (1) describes the change of magnetization due to the external magnetic field. Within a certain time constant, it drives the direction of the magnetic moment into the field direction. The term containing the random torques describes the relaxation into equilibrium. Figure 2 shows a numerical solution of equation (1) with respect to the mean magnetic moment for the two limiting cases. For the parameters chosen, the field-induced rotation dominates the thermal relaxation.

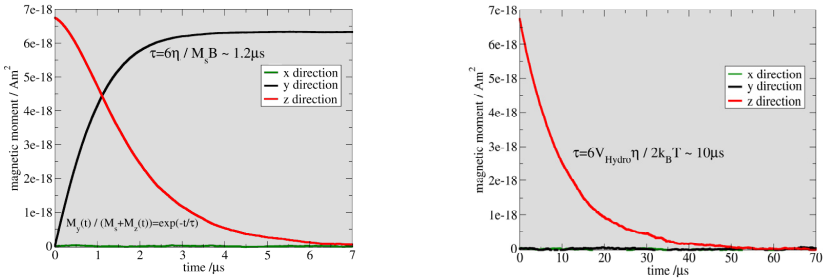


**Fig. 2.** Calculated single particle mean magnetic moment for  $10^4$  particles of 30nm diameter, with  $\eta=1$  mPa s,  $M_s=0.6T/\mu_0$  at  $T=300K$ . At  $t=0s$  all particles are aligned in z direction. On the left side a constant field of  $B=10mT$  is applied in y direction at  $t=0$  s. On the right side, no magnetic field is present. The theoretical time constants  $\tau$  are taken from<sup>12</sup>.

If an oscillating magnetic field is applied, both time constants will be noticeable. Relaxation will take place for small field values and rotation towards the field direction will dominate for large fields. If the change of the external magnetic field is faster than the internal time constants, a delay of magnetization alignment with respect to the field will occur. This fact is illustrated in figure 3, where 1000 solutions of equation (1) are visualized. Each dot represents the tip of a single particle magnetization vector  $M_s \vec{n}$ , projected to the xy-plane for  $T=300$  K. At the very beginning, all particles are aligned in vertical direction (y-direction). The orange line is the mean value of the magnetization. Some dephasing due to thermal relaxation can already be seen after a few microseconds in the upper left image. An oscillating magnetic field in horizontal direction (x-direction) with frequency  $f=1/T=25$  kHz<sup>5,13</sup> is switched on, as indicated by the green line. With increasing field, the particles are forced to rotate in the direction of the field (see first row, second image). After  $t=T/4$ , the magnetic field amplitude decreases, but due to the time constants  $\tau$ , the magnetization remains aligned, even if the magnetic field passes zero (see second row, second image). Finally, the magnetic field increases in the negative direction forcing the particles to rotate back in field direction. At some point in time, the total magnetization will therefore be zero, indicating that a hysteresis loop is passed by the magnetization (second row, last image and third row). This process of relaxation and delayed magnetization alignment will occur periodically and after some cycles an equilibrium state will be reached. The width of the hysteresis loop will depend on the time constant  $\tau$ , the frequency  $\omega=2\pi f$  and the temperature  $T$ .

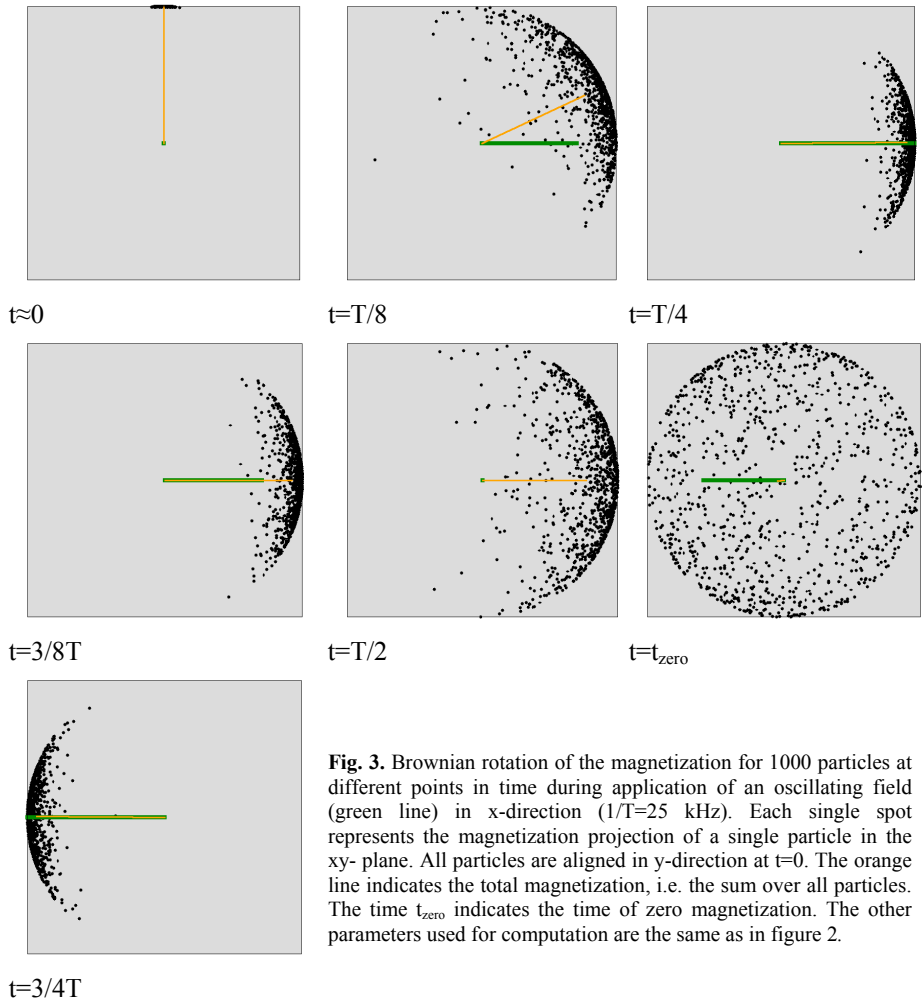


**Fig. 3.** Brownian rotation of the magnetization for 1000 particles at different points in time during application of an oscillating field (green line) in  $x$ -direction ( $1/T=25$  kHz). Each single spot represents the magnetization projection of a single particle in the  $xy$ -plane. All particles are aligned in  $y$ -direction at  $t=0$ . The orange line indicates the total magnetization, i.e. the sum over all particles. The time  $t_{\text{zero}}$  indicates the time of zero magnetization. The other parameters used for computation are the same as in figure 2.

For sufficiently low frequencies, the hysteresis loop will collapse into the Langevin-Theory, as the thermodynamic equilibrium is maintained at each point in time. Figure 4 shows the hysteresis loops for different cases. Obviously, the magnetization behaviour depends sensitively on the particle diameter and the ratio of frequency and viscosity. As the steepness of the magnetization curve determines the spatial resolution for MPI, the hysteresis loop is of particular interest.

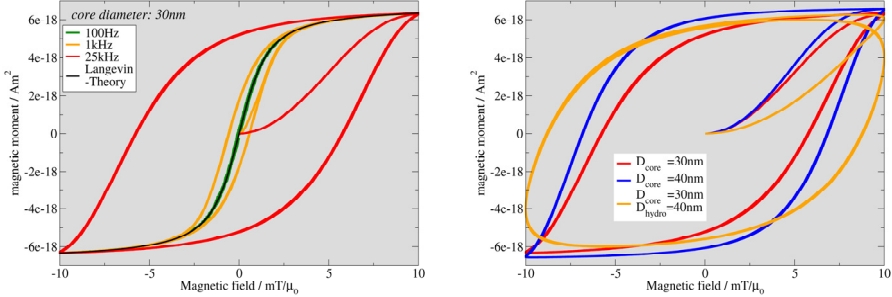


**Fig. 4.** Mean magnetic moment in field direction as function of the external magnetic field (x-direction). At  $t=0$ , all particles are aligned in y-direction. On the left side, the frequency and on the right side the core and hydrodynamic diameter of the particles are varied (for the red and blue line hydrodynamic and core diameter are the same). Ten periods are shown in order to see the convergence to the equilibrium state. The other parameters are the same as in figure 2. The data for 40 nm particles (right side) are scaled to those of the 30 nm particles for comparability.

Obviously, the steepness decreases for higher frequencies and for particles with coating (figure 4). At 25 kHz, the contribution to the MPI signal due to Brownian rotation is restricted to the low frequency regime, as can be seen by comparing the steepness of the corresponding hysteresis loop with Langevin-Theory, as expected for Néel rotation. Therefore, the theoretical treatment of the magnetization change due to Néel rotation will be briefly sketched.

### 2.2. Néel Rotation

As already mentioned in the context of figure 1, the magnetic moment may change its direction due to an external magnetic field or due to relaxation to the equilibrium state. If thermal noise is included, like in equation 1, the deterministic equation translates to a Langevin equation. This equation is well known in micro-magnetics and called Landau-Lifschitz-equation. The time evolution of the magnetization  $\vec{M}$  for a single particle is given by<sup>2</sup>.

$$\frac{d\vec{M}}{dt} = -\frac{\gamma}{(1 + \alpha^2)} \left\{ \vec{M} \times (\vec{B}_{total}(t) + \vec{\mathcal{B}}(t)) - \frac{\alpha}{M_s} \vec{M} \times [\vec{M} \times (\vec{B}_{total}(t) + \vec{\mathcal{B}}(t))] \right\}$$

Here,  $\vec{B}_{total}$  is the deterministic magnetic field the particle is exposed to,  $\gamma$  is the gyromagnetic ratio of the particle,  $\alpha$  is a damping constant, and  $M_s$  is the saturation magnetization of the particle. Thermal noise is taken into account via a

fluctuating magnetic field  $\vec{\mathcal{B}}$ . The properties of this stochastic field are according to the dissipation-fluctuation theorem

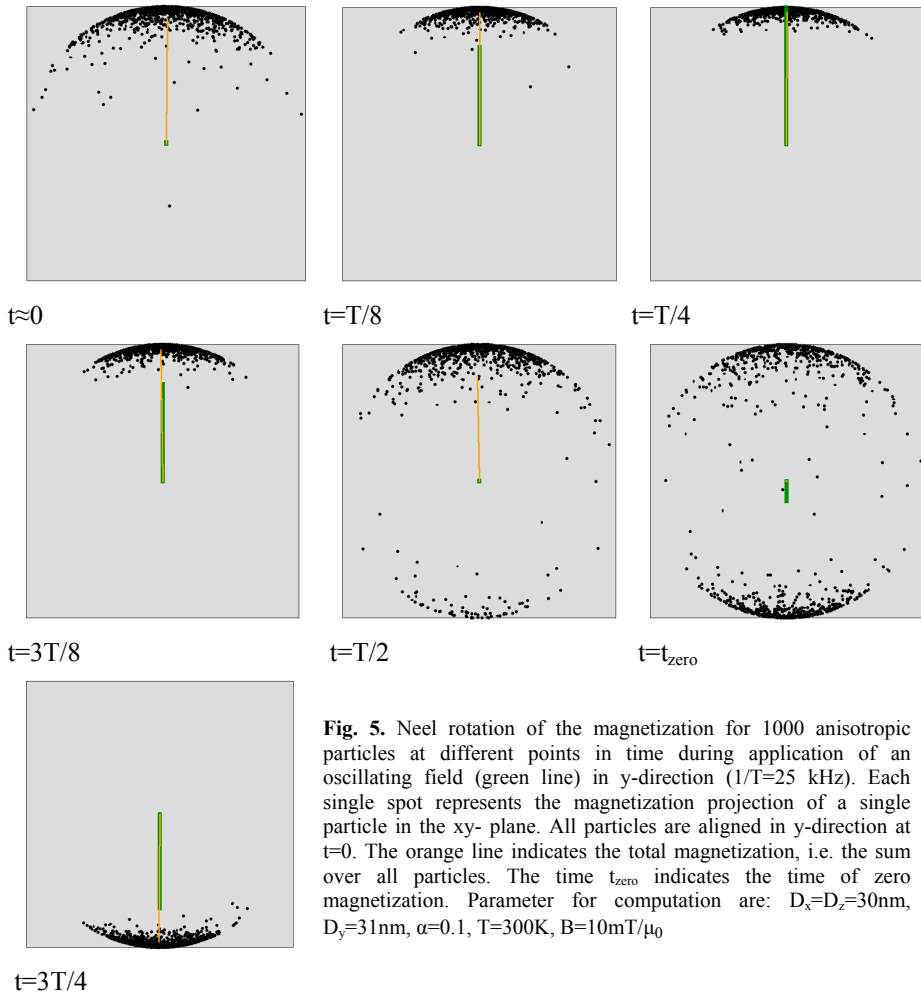
$$\langle \vec{\mathcal{B}}_i(t) \rangle = 0 \quad \langle \vec{\mathcal{B}}_i(t) \vec{\mathcal{B}}_j(t') \rangle = \frac{2\alpha k_B T}{\gamma M_s V_{core}} \delta(t-t') \delta_{ij} \quad i, j = 1, 2, 3$$

As already mentioned, the numerical solution of these types of equation depends on the calculus used. Again, the Stratonovitch interpretation is chosen and a Heun<sup>11</sup> scheme for the numerical solution of the above equation is used. In this case, however, the additional diffusion term after transformation can be omitted<sup>1,9</sup>.

In  $\vec{B}_{total}$ , all contributions to the magnetic field, like external magnetic field, crystal field or demagnetization field, are included. In this paper, only an external magnetic field and axial field anisotropy due to the shape of the particle are taken into account. Already a small change of the large magnetic core diameter preferred in MPI in one direction induces an anisotropy comparable to the drive fields, as will be seen shortly. Hence, the total magnetic field can be written as

$$\vec{B}_{total}(t) = \vec{B}_{ext}(t) - \mathbf{D} \cdot \vec{M}$$

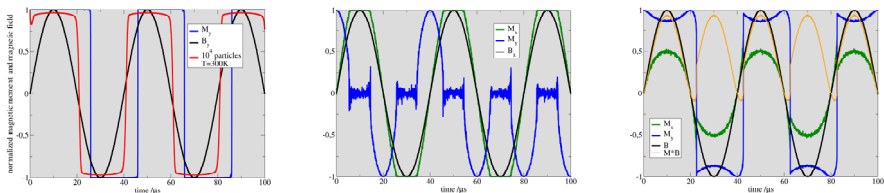
The Matrix  $\mathbf{D}$  represents the demagnetization tensor and contains the demagnetizations factors  $N_x, N_y, N_z$  on its diagonal if written in the principal axis system<sup>10</sup>. If the total magnetic field is substituted into equation (2), its numerical solution is comparable to the case of Brownian rotation. The respective analysis of the magnetization of 1000 single ellipsoidal particles with aspect ratio 31/30 is shown in figure 5.



**Fig. 5.** Neel rotation of the magnetization for 1000 anisotropic particles at different points in time during application of an oscillating field (green line) in y-direction ( $1/T=25$  kHz). Each single spot represents the magnetization projection of a single particle in the xy- plane. All particles are aligned in y-direction at  $t=0$ . The orange line indicates the total magnetization, i.e. the sum over all particles. The time  $t_{zero}$  indicates the time of zero magnetization. Parameter for computation are:  $D_x=D_z=30\text{nm}$ ,  $D_y=31\text{nm}$ ,  $\alpha=0.1$ ,  $T=300\text{K}$ ,  $B=10\text{mT}/\mu_0$

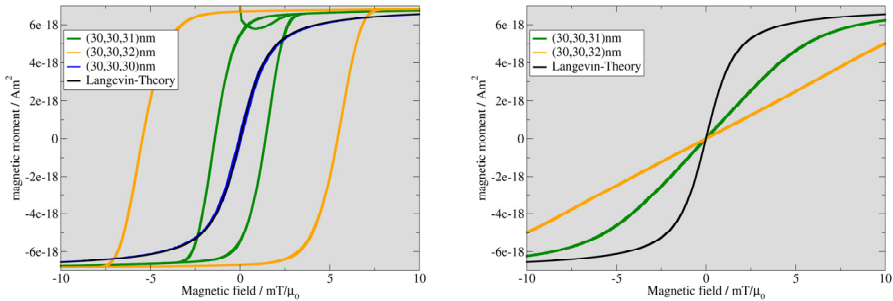
After a short decay, the magnetization is pinned in the direction of the anisotropy axis (vertical). At zero external magnetic field, the total magnetization remains aligned in that direction. After  $t=T/2$ , the magnetic field is reversed and the amount of particles overcoming the energy barrier with thermal assistance increases. The height of the energy barrier depends on the anisotropy of the particles. At a certain field the magnetization passes zero and the particles are equally distributed in both directions. Finally, the magnetization is again aligned vertically, but now in the opposite direction. Figure 6 shows the same process as in

figure 5 for a single particle and different field directions. The thermal noise was suppressed by choosing  $T=1$  K for better illustration. On the left side, the situation is similar to figure 5. For comparison, the single particle mean value at 300 K is also plotted. For a single particle, the magnetization reverses at the anisotropy field  $B_{aniso}$ , i.e. at about  $7.8 \text{ mT}/\mu_0$ , which is for axial symmetry  $M_s(N_y - N_x)^{1/4}$ . Obviously, the mean magnetization at elevated temperatures flips at lower fields ( $\sim 1.4 \text{ mT}/\mu_0$ ) due to thermally assisted barrier hopping (see also figure 5). If the field is aligned in horizontal direction (central graph, figure 6), the magnetic moment rotates from the axial (vertical) direction into the horizontal field direction. At the anisotropy field, the magnetization is aligned and rests in horizontal direction. If the field is lowered, both states, magnetization up or down, are equally likely (see non-periodically flips in blue line), so the magnetization will show no hysteresis effects in that direction. The right graph in figure 6 shows the magnetization dynamics if the field is aligned at  $50^\circ$  with respect to the vertical (axial) direction. So, again, the magnetization rotates in field direction. There remains, however, a certain angle between field and magnetization direction (see orange line).



**Fig. 6.** Single particle dynamics for ellipsoidal particles with aspect ratio of 31nm to 30nm at low temperatures (1 K). On the left side, the field is directed into the vertical (axial) direction. The red line represents the mean value for  $10^4$  particles at 300 K. In the central graph, the field is perpendicular to the anisotropy (axial) axis. On the right side, the field is applied at an angle of  $50^\circ$  to the axial direction. The orange line represents the cosine of the angle between magnetization and magnetic field.

For the resolution in MPI the steepness of the magnetization curve is important, so the mean particle magnetization can also be plotted as a function of the magnetic field. This is shown for  $10^4$  particles for vertical (axial) and horizontal field directions in figure 7, beginning at  $t=0$ .



**Fig. 7.** Mean magnetic moment in field direction as function of external magnetic field for parallel (left) and perpendicular field direction with respect to the axial direction. At  $t=0$  the magnetization is aligned in axial direction. The calculated anisotropy fields are  $7.8 \text{ mT}/\mu_0$  and  $15.3 \text{ mT}/\mu_0$  for aspect ratios of  $31/30$  and  $32/30$ , respectively. For  $300 \text{ K}$ , the width of the loops is lower than the anisotropy fields ( $2.8 \text{ mT}/\mu_0$  and  $10.8 \text{ mT}/\mu_0$ , respectively).

As anticipated, for field variations in the direction of the anisotropy, a hysteresis loop is present, whereas for the direction perpendicular to this axis, the magnetization crosses the origin. In addition, the steepness in the left graph is much higher compared to the right one, which can be validated by comparison to a  $30 \text{ nm}$  particle according to Langevin-Theory. So, in an MPI experiment, only a low signal from the direction perpendicular to the axial direction would be expected from these results. A larger anisotropy leads to larger hysteresis loops, e.g. a change of  $+2 \text{ nm}$  for a  $30 \text{ nm}$  particle leads to a hysteresis width on the order of the applied field. Clearly, particles with a mean anisotropy field larger than the drive field amplitude will not contribute to an MPI signal. Finally, comparing figure 7 and figure 4 indicates, that for axial alignment only the Néel process contributes to the MPI signal.

### 2.3. Combined Rotation

The combination of both causes of magnetization change is described by solving equation (1) and (2) simultaneously. The coupling between both equations is due to the magnetic torque in the first equation and the non-diagonal demagnetization tensor in the second equation. In the following the vector  $\vec{n}$  points always in the direction of the easy axis (axial direction), which will in general be different from the direction of the magnetization. Therefore, a substitution according to

$$(M_s \vec{n} \times \vec{B}) \times \vec{n} \rightarrow (\vec{M} \times \vec{B}) \times \vec{n} \text{ and } \mathbf{D} \rightarrow \mathbf{D}(\vec{n})$$

is performed and a numerical solution is obtained as already described.

Figure 8 illustrates the dynamics of a single particle at  $T=1$  K. The left graph shows the magnetization vector and the vector  $\vec{n}$  (axial direction) as a function of time, after an oscillating magnetic field in horizontal direction has been applied.

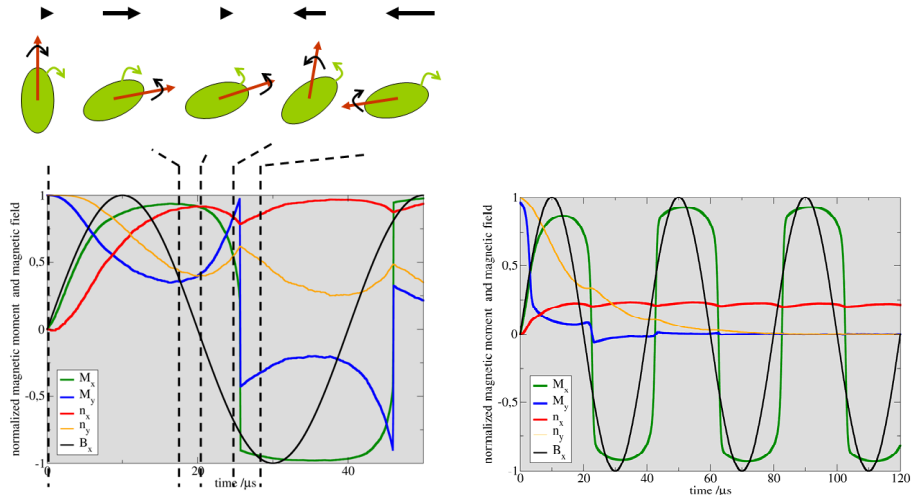


**Fig. 8.** Magnetization and rotational dynamics of a single particle at  $T=1$  K (left side). On the right side, the mean value over  $10^4$  particles at 300 K is plotted. The axial anisotropy is represented by a diameter deviation of +2 nm for a 30 nm particle. The viscosity is 5 mPa s, the amplitude of the oscillating magnetic field is  $10 \text{ mT}/\mu_0$  at 25 kHz. The green ellipses and red arrows above the left graph indicate the direction of rotation of the particle and the magnetization. The black arrows indicate the direction and field strength.

The magnetization as well as the axial direction at  $t=0$  was directed in positive  $y$ -direction (vertical). The green ellipses (particle) and the red arrows (magnetization) above the graph illustrate the dynamics of the rotation at different points in time, indicated by the dashed lines. At the very beginning, the magnetization as well as the particle rotates into the field direction, until a minimum vertical magnetization is reached. At that point, the external field is too low to further rotate the particle, so it starts rotating back into axial direction. At  $B_{\text{ext}}=0$ , the magnetization is aligned in axial direction ( $\vec{n} \parallel \vec{M}$ ), which is the state of lowest energy and, thus,  $n_y$  reaches its minimum value. Afterwards, the field amplitude increases in negative  $x$ -direction, so the single particle magnetization further rotates in positive  $y$ -direction, as does  $n_y$ . If, finally, the magnetization exhibits a negative

x-direction component due to the external magnetic field, the vector  $\vec{n}$  will again change direction, to align itself in magnetization direction. This process will continue until all particles are aligned horizontally. This can be seen from the right side of figure 8. Again,  $10^4$  particles at 300K have been averaged. As expected, the magnetization does not flip at zero field, and again, a hysteresis loop is expected. This is confirmed in figure 9, right side. The mean particle magnetization is plotted after ten periods versus the external magnetic field and compared to exclusive Néel rotation (see also figure 7) and the case of an additional hydrodynamic diameter. After the equilibrium state (particles aligned horizontally) is reached, there is almost no difference between coated and uncoated particles. However, the magnetization curve differs significantly from the case of exclusive Néel rotation. As a consequence, a lower signal for the combined rotation would be expected. This can also be seen on the left side (of figure 9), where the magnetization as function of time is plotted. The reason is the dephasing of the particles due to Brownian rotation at low magnetic field values. It was furthermore checked, that for large viscosities the Néel limit is reproduced.

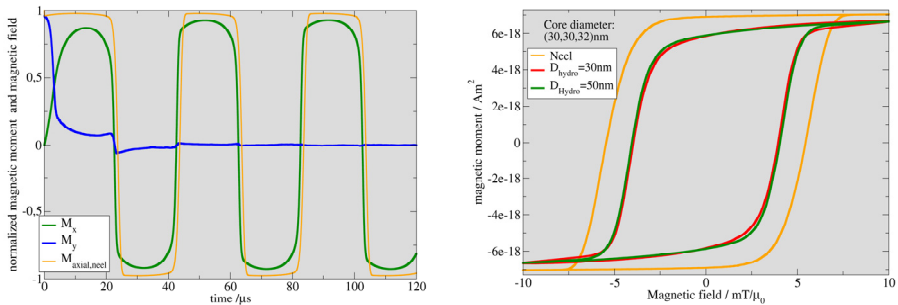


**Fig. 9.** The mean magnetic moment of  $10^4$  particles at  $T=300$  K for the combined rotation. Left side: time evolution compared to exclusive Néel rotation; right side: the subsequent hysteresis loop. Additionally, the case for coated particles is also shown. In equilibrium there is only little difference, whereas the transient response (not shown) clearly differs due to different Brownian rotational time constants

### 3. CONCLUSION

In this paper, a detailed theory of Brownian, Néel and combined rotation of magnetic monodomain particles in the context of MPI was presented. A Langevin equation for the Brownian and Néel rotation was numerically solved. The relevant parameters like frequency, viscosity, particle diameter and anisotropy were chosen to apply to Magnetic Particle Imaging. It turned out, that the Néel process provides the main contribution to the MPI signal. The Brownian rotation, however,

significantly influences the signal strength, even for magnetic fields directed permanently in axial direction. A small but defined anisotropy is acceptable, as the magnetization can be flipped with the external field. However, small diameter deviations induce substantial anisotropy fields.

## REFERENCES

- 1 Gleich B, Weizenecker J, *Nature* 2005, **435**, p. 1214
- 2 Weizenecker J, Borgert J, Gleich B, *Phys Med Biol* 2007, **52**, p. 6363-6374
- 3 Knopp T, Biederer S, Sattel T F, Weizenecker J, Gleich B, Borgert J, Buzug TM, *Physics in Medicine and Biology*, 2009, **54/2**, p 385
- 4 Knopp T, Biederer S, Sattel TF, Weizenecker J, Gleich B, Borgert J, Buzug TM, *Bildverarbeitung für die Medizin*, 2010, Springer, 1-5.
- 5 Engel A, Reimann P, *Phys. Rev. E*, 2004, **70**, 051107
- 6 Coffey WT, Kalmykov YP, Waldron JT, *The Langevin Equation*, World Scientific (2004).
- 7 Kloeden PE, Platen E, *Numerical Solution of Stochastic Differential Equations*, Springer-Verlag (1999)
- 8 Scholz W, Schrefl T, Fidler J, *J. Magn. Magn. Mater.*, 2001, **233**, p. 296
- 9 Valberg PA, Butler JP, *Biophys. J.* 1987, **52** p. 537
- 10 Brown WF Jr, *Phys. Rev.*, 1963, **130**, p. 1677
- 11 Berkov DV, Gorn NL, *J. Condens. Matter*, 2002, **14**, p. L281
- 12 Martinez E, Lopez-Diaz L, Torres L, Alejos O, *Physica B*, 2004, **343**, p. 252
- 13 Osborn JA, *Phys. Rev.*, 1945, **67/11**, p. 12
- 14  $E_{demag} = -\vec{M}^T \mathbf{D} \vec{M} = M_s \sin^2(\theta) M_s (N_z - N_x) + \frac{1 - N_z}{2} M_s^2 = M_s \sin^2(\theta) B_{aniso} + E_0$